Structure of the Binuclear Iron Center in Hemerythrin by X-ray Absorption Spectroscopy

W. T. Elam,[1a] E. A. Stern,*[1a] J. D. McCallum,[1b] and J. Sanders-Loehr[1b]

Contribution from the Physics Department, FM-15, University of Washington, Seattle, Washington 98195, and the Chemistry Department, Portland State University, Portland, Oregon 97207. *Received December 21, 1981*

Abstract: Iron K-edge X-ray absorption data, including the near-edge structure and the extended X-ray absorption fine structure (EXAFS), have been measured for the respiratory protein hemerythrin in the biologically active oxy and deoxy forms of hemerythrin as well as metazido- and methydroxohemerythrin. The active-site structure is found to be very similar in the oxy and met forms, but distinctly different in deoxyhemerythrin. The binuclear iron center in oxy- and methemerythrins contains a μ-oxo bridge similar to Fe_2O-containing standard compounds. The EXAFS data for metazidohemerythrin indicate that the average iron environment consists of a total of five nitrogen and oxygen ligands at 2.15 ± 0.05 Å and a bridging oxygen at 1.80 ± 0.08 Å, implying a bridging bond angle of 152 (+28/−13)°. Deoxyhemerythrin shows distinct changes in the first-shell EXAFS, and the iron–iron peak has disappeared, indicating loss of the μ-oxo bridge upon reduction.

Hemerythrin is a respiratory protein found in the coelomic fluid of a number of marine invertebrates. The active site of the protein contains two non-heme iron atoms that reversibly bind one molecule of oxygen. The iron in deoxyhemerythrin is in the ferrous state. Formation of oxyhemerythrin results in the oxidation of both iron atoms to an antiferromagnetically coupled ferric state with concomitant reduction of dioxygen to peroxide. Replacement of the bound peroxide by anions such as azide or hydroxide leads to methemerythrins in which the two Fe(III) ions retain their antiferromagnetic coupling but are no longer functional in transporting oxygen.[2,3]

Several met forms of hemerythrin and the analogous muscle protein, myohemerythrin, have been the subjects of X-ray crystallographic investigations.[4,5] The proposed active-site structure based on 2.2-Å resolution data for metazidohemerythrin[6] is shown in Figure 1. A salient feature of this structure is that the iron atoms are bridged by two protein carboxylates and an oxo group derived from solvent. The μ-oxo bridge had long been predicted on the basis of spectroscopic and magnetic behavior[2] and has been independently verified in methemerythrin by resonance Raman studies of oxygen isotope exchange.[7] Since the μ-oxo bridge is presumed to be also present in oxyhemerythrin, it is likely that the bound peroxide resides in the same location as the azide ion in metazidohemerythrin. However, the difficulty of producing crystals of the more biologically important oxy and deoxy forms of hemerythrin has so far prevented a definitive answer to this question.

X-ray absorption spectroscopy offers another technique for obtaining direct information on the structure of the iron center in hemerythrin. The extended X-ray absorption fine structure (EXAFS) past the absorption edge is an interference effect caused by backscattering of the X-ray photoelectron by neighboring atoms. It can be directly analyzed to give radial interatomic distances and the number and types of ligands around the absorbing atom. EXAFS is particularly suited for studies on metalloproteins as the environment surrounding the heavy atom can be focused on by tuning the X-rays to the atom's absorption edge. Unlike X-ray diffraction, the structure can be determined independently of the physical state of the protein, e.g., in solution. Previous studies on the iron-containing core of ferritin, for example, led to the assignment of the iron atoms in this polymer to a distorted octahedral arrangement in which each iron atom was surrounded by 6.4 ± 0.6 oxygens at a distance of 1.95 Å in the first coordination shell and 7 ± 1 iron atoms at a distance of 3.29 Å in the second coordination shell.[8] We have obtained data on the Fe K absorption edge and EXAFS for oxyhemerythrin and deoxyhemerythrin as well as metazidohemerythrin and methydroxohemerythrin. Our results show that the structure of the iron complex in oxyhemerythrin is very close to that of the met forms and distinctly different from that of deoxyhemerythrin.

Experimental Section

Hemerythrin. Hemerythrin was obtained from the sipunculid *Phascolopsis gouldii* as described previously.[9] Methemerythrin was prepared by treatment with a twofold excess of $K_3Fe(CN)_6$ followed by extensive dialysis vs. 0.1 M Tris-SO_4 (pH 8.9) to form methydroxohemerythrin or 0.1 M Tris-SO_4, 0.01 M NaN_3 (pH 7.5) to form metazidohemerythrin. Deoxyhemerythrin was prepared from methydroxohemerythrin by anaerobic dialysis vs. sodium dithionite (twofold molar excess to Fe) followed by anaerobic dialysis vs. 0.1 M Tris-SO_4 (pH 8.1). Oxyhemerythrin was formed by exposing deoxyhemerythrin to air 30 min prior to use of the sample in order to minimize the extent of autooxidation of oxyhemerythrin to methemerythrin. Methemerythrin samples were concentrated by ultrafiltration. Sample concentrations were 0.016 M in Fe (metazido form) and 0.0075 M in Fe (methydroxo, oxy, and deoxy forms) on the basis of ϵ_{280} = 17 700 M^{-1} cm^{-1} per Fe.[10]

Standard Compounds. Iron foil was obtained from Alfa Products. The Fe(glycine) trimer, $[Fe_3O(\text{glycinato})_6(H_2O)_3](ClO_4)_7$, was prepared and characterized as described previously.[8] The Fe(Cl(PDC)) dimer, $[Fe_2O(\text{4-chloro-2,6-pyridinedicarboxylate})_2(H_2O)_4]\cdot 4H_2O$, was a gift of Dr. H. J. Schugar. This material had been characterized by X-ray crystallography.[11] The Fe(TIM) compound, bis(acetonitrile)(2,3,9,10-tetramethyl-1,4,8,11-tetrazacyclotetradeca-1,3,8,10-tetraene)iron(II) hexafluorophosphate, was kindly supplied and characterized by Dr. Norman Rose.

X-ray Absorption. X-ray absorption measurements were performed at the Stanford Synthrotron Radiation Laboratory at room temperature by using the wiggler line. The absorption by the iron atoms in the protein samples was monitored via the iron Kα fluorescent emission using a filter and Soller slit assembly[12] coupled to a low-noise ion chamber.[13] The

(1) (a) University of Washington. (b) Portland State University.
(2) Loehr, J. S.; Loehr, T. M. *Adv. Inorg. Biochem.* **1979**, *1*, 235–252.
(3) Kurtz, D. M., Jr.; Shriver, D. F.; Klotz, I. M. *Coord. Chem. Rev.* **1977**, *24*, 145–178.
(4) Stenkamp, R. E.; Jensen, L. H. *Adv. Inorg. Biochem.* **1979**, *1*, 219–233.
(5) Hendrickson, W. A. *Nav. Res. Rev.* **1978**, *31*, 1–20.
(6) Stenkamp, R. E.; Sieker, L. C.; Jensen, L. H.; Sanders-Loehr, J. *Nature (London)* **1981**, *291*, 263–264.
(7) Freier, S. M.; Duff, L. I.; Shriver, D. F.; Klotz, I. M. *Arch. Biochem. Biophys.* **1980**, *205*, 449–463.
(8) Heald, S. M.; Stern, E. A.; Bunker, B.; Holt, E. M.; Holt, S. L. *J. Am. Chem. Soc.* **1979**, *101*, 67–73.
(9) Klotz, I. M.; Klotz, T. A.; Fiess, H. A. *Arch. Biochem. Biophys.* **1957**, *68*, 284–299.
(10) Dunn, J. B. R.; Addison, A. W.; Bruce, R. E.; Loehr, J. S.; Loehr, T. M. *Biochemistry* **1977**, *16*, 1743–1749.
(11) Ou, C. C.; Wollmann, R. G.; Hendrickson, D. N.; Potenza, J. A.; Schugar, H. J. *J. Am. Chem. Soc.* **1978**, *100*, 4717–4724.
(12) Stern, E. A.; Heald, S. M. *Rev. Sci. Instrum.* **1979**, *50*, 1579–1582.
(13) Stern, E. A.; Elam, W. T.; Bunker, B. A.; Lu, K. Q.; Heald, S. M. *Nucl. Instrum. Method* **1982**, *195*, 345–346.

0002-7863/82/1504-6369$01.25/0

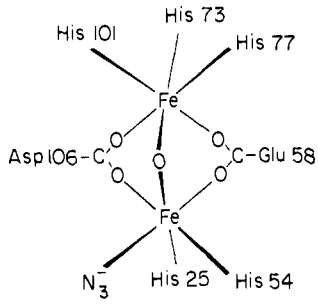

Figure 1. Structure based on X-ray crystallographic measurements of the active site in metazidohemerythrin. Reprinted with permission from ref 6. Copyright 1981, Macmillan.

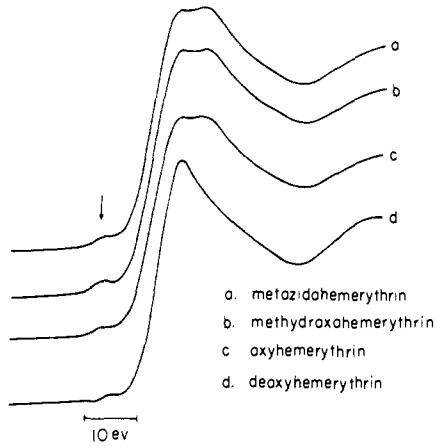

Figure 2. X-ray absorption data showing the structure near the iron K edge in the various forms of hemerythrin. All are similar except for deoxyhemerythrin, consistent with the change from +3 to +2 oxidation state upon reduction. The arrow points to the 3d pip resulting from weak transitions to unfilled 3d levels on the iron atoms. The edges have been shifted by arbitrary amounts to align the first peak above the edge.

standard compound measurements were done in transmission. Data for each sample were collected as a series of scans, each taking 10 min and yielding more than 10^6 counts per data point. Scans were repated until an overall statistical signal to noise ratio of 3×10^3 or better was achieved. In general, four scans were adequate and no change in signal was observed between the first and the last scan. The methemerythrin and oxyhemerythrin samples exhibited normal color before and immediately after measurement, while the deoxyhemerythrin sample remained colorless. Addition of air to the deoxyhemerythrin sample after exposure to X-rays resulted in the appearance of the normal amount of red color characteristic of oxyhemerythrin, indicating that the sample was still intact. Subsequent analysis of the optical absorption spectra[14] of these samples 4 days after exposure to X-rays showed that the metazidohemerythrin and methydroxohemerythrin maintained 100% integrity. The oxyhemerythrin sample retained 95% activity and contained less than 10% methemerythrin. The deoxyhemerythrin sample had only 75% of its original activity 4 days after irradiation. Protein precipitation also became apparent, though it was not present immediately after irradiation. An important factor in maintaining sample integrity was the use of Teflon cells; considerable protein denaturation was observed when samples were placed in conventional brass cells.

Results

Near-Edge Structure. The near-edge structure within approximately 20 eV of the K edge of Fe contains information on the oxidation state and coordination geometry of the iron atoms, while the EXAFS region containing structure information begins approximately 40 eV past the edge. Near-edge structures for the four forms of hemerythrin are shown in Figure 2. Metazidohemerythrin, methydroxohemerythrin, and oxyhemerythrin all have edge structures characteristic of Fe(III) complexes and similar to those observed with the Fe(III)–O–Fe(III) standards: the Fe(Cl(PDC)) dimer and the Fe(glycine) trimer. Deoxyhemerythrin has a markedly narrower edge structure such as that of ferrous oxalate and thus is clearly an Fe(II) species.

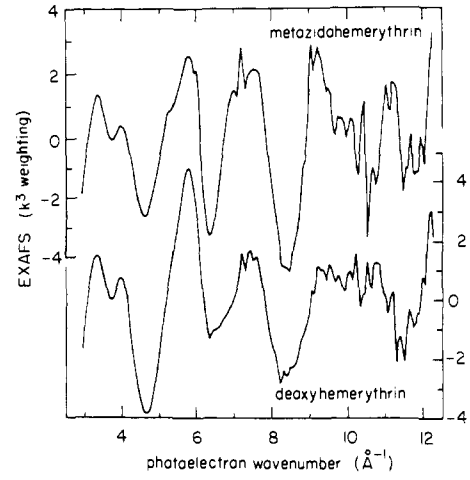

Figure 3. Oscillatory EXAFS above the iron K edge in metazidohemerythrin and deoxyhemerythrin. The data have had the background removed and the abscissa converted from energy to electron wavenumber k and multiplied by k^3 to offset the decreasing amplitude at high k. The data for oxy- and methydroxohemerythrin are very similar to that for metazidohemerythrin. Some differences in the deoxyhemerythrin data are visible by eye.

A detail of the absorption edge that has structural significance is the 3d "pip" shown by the arrow in Figure 2. This feature is due to transitions to unoccupied 3d states on the iron atom. Such transitions are formally forbidden by dipole selection rules for an inversion symmetric environment. However, a weak quadrupole absorption is allowed and is further enhanced by inversion asymmetry in the iron environment.[15] For example, the pip intensity is enhanced for tetrahedrally coordinated iron atoms as in rubredoxin.[16] The hemerythrin samples have a relatively large pip intensity for six ligands. The intensity is increased in going from the ferrous deoxyhemerythrin forms to the ferric forms (oxyhemerythrin to metazidohemerythrin), indicating that all three forms of the protein have a strongly inversion–asymmetric octahedral geometry about the two iron atoms. This is in agreement with the active-site structure of metazidohemerythrin determined by X-ray crystallography (Figure 1), which contains a short bond at the μ-oxo bridge. The noticeably largest pip for methydroxohemerythrin implies that this form of the protein has the most inversion–asymmetric arrangement around one or both of the iron atoms.

Extended X-ray Absorption Fine Structure. Analysis of EXAFS data above the iron absorption edge in the hemerythrin samples was undertaken to gain a more detailed knowledge of the location of atoms around the iron. These data were compared with those from several well-characterized standard compounds to obtain the structural information.

An example of the oscillatory EXAFS $\chi(k)$ above the iron absorption edge is shown in Figure 3 for metazidohemerythrin and for deoxyhemerythrin. Some differences are apparent even at this level of analysis. A Fourier transform of the EXAFS spectrum is more easily interpreted because it provides information on the locations of various shells of atoms surrounding the absorbing iron atom. The contributions of heavier atoms extend to higher k values and can be amplified by a k^3 weighting in the Fourier transforms. Such transforms are presented in Figure 4 for the four forms of hemerythrin and the standard Fe(Cl(PDC)) dimer and Fe(glycine). Most transforms contain three distinct peaks that are delineated by brackets. By backtransforming the region within each peak into k space, its contribution to the EXAFS can be isolated. The oscillations contributing to the second peak have a minimum amplitude at $k = 5$ Å^{-1} and a

(14) Garbett, K.; Darnell, D. W.; Klotz, I. M.; Williams, R. J. P. *Arch. Biochem. Biophys.* **1969**, *135*, 419–434.

(15) Bain, R. A.; Goodard, W. A., III. *Phys. Rev. B: Condens. Matter* **1980**, *22*, 2767–2776.

(16) Bunker, B.; Stern, E. A. *Biophys. J.* **1977**, *19*, 253–264.

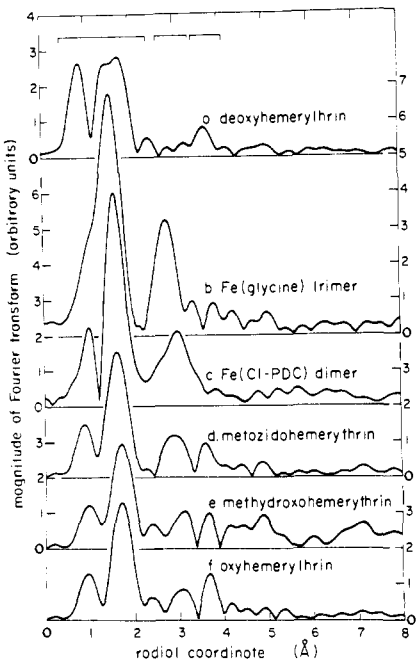

Figure 4. Fourier transforms of the EXAFS oscillations above the iron K edge in the various forms of hemerythrin and in the Fe(Cl(PDC)) dimer and the Fe(glycine) trimer. The radial coordinate is not corrected for the effects of atomic potentials. Oscillations over the range of 3–12 Å^{-1} in k space were included, and the data were weighted by k^3 to provide approximately constant amplitude over this range. Inclusion of data beyond 12 Å^{-1} introduces unacceptable noise.

Table I. Comparison of Iron-Iron Distances Determined by EXAFS and X-ray Diffraction

sample	Fe–Fe distance, Å		Fe–O–Fe angle, deg
	EXAFS[a]	crystallogr.	
Fe(glycine) trimer	3.31 ± 0.05	3.30[b]	120[b]
Fe(Cl·(PDC)) dimer	3.48 ± 0.05	3.54[c]	180[c]
metazidohemerythrin	3.49 ± 0.08	3.30[d]	152 (+28/−13)
methyldroxohemerythrin	3.54 ± 0.08		153 (+27/−13)
oxyhemerythrin	3.57 ± 0.08		155 (+25/−13)

[a] Determined by reference to the following standards: iron foil for Fe(glycine) trimer; Fe(glycine) trimer for Fe(Cl·(PDC)) dimer; Fe(glycine) trimer for hemerythrins. [b] Reference 27. [c] Reference 11. [d] Reference 31.

maximum at k = 8.5 Å^{-1}. This is characteristic of iron backscattering as observed in the standard compounds. This can be compared with the first and third peaks, which are composed of lower atomic-weight atoms and have maximum amplitude at about k = 6 Å^{-1}. Deoxyhemerythrin is distinguished by its lack of an Fe–Fe peak.

Iron–Iron Distance. Iron–iron distances can be obtained by comparing the phase and amplitude of the oscillations giving rise to the iron–iron peak with similar signals from known compounds.[17] Table I shows calculated iron–iron distances for the hemerythrin samples obtained by comparison with the Fe(glycine) trimer. The quoted errors are based on statistical fluctuations and the lack of consistency among the standards for determining the Fe–Fe distance. With iron foil and/or the Fe(glycine) trimer as models, the distances obtained for the Fe(Cl(PDC)) dimer is in error by 0.06 Å. This difference is expected because of the strong perturbation introduced by the intervening oxygen in the μ-oxo bridge that is in a straight line with the center and backscattering irons. As first pointed out by Lee and Pendry,[18] this shadowing enhances the amplitude of the Fe peak and perturbs the apparent distance.[19] The measured enhancement of shadowing

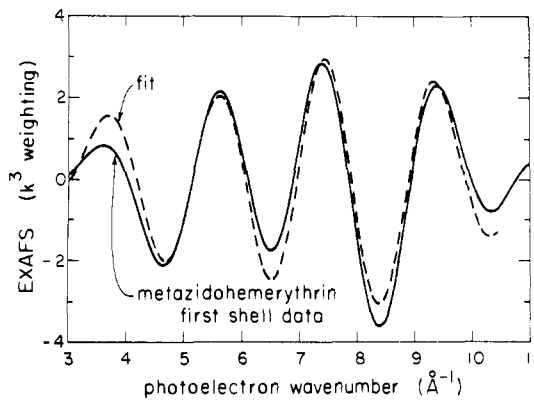

Figure 5. The solid line is the first-shell EXAFS in metazidohemerythin obtained by backtransforming over the range delineated in Figure 4. The dashed curve is the best fit to the data. The fitting procedure is detailed in the text and the resultant parameters are summarized in Table II.

of the amplitude in the Fe(Cl(PDC)) dimer was about two relative to the Fe(glycine) trimer. This can be seen in Figure 4 since the trimer has two iron neighbors while the dimer has only one, yet their iron–iron peaks are about equal. The hemerythrins also do not show this amplitude enhancement, suggesting that Fe(glycine) is a better standard than Fe(Cl(PDC)).

There is a significant disagreement between EXAFS and X-ray crystallography in the Fe–Fe distance in metazidohemerythrin that deserves further study to resolve. The iron–iron distances in oxyhemerythrin and methydroxohemerythrin may be somewhat larger than in metazidohemerythrin, but the difference is not outside the errors. The deoxyhemerythrin structure must be distinctly different from that of the oxidized forms because no iron–iron peak is apparent in the EXAFS Fourier transform.

First Coordination Shell. The first and strongest peak in all of the transforms (Figure 4) is the signal from the first coordination shell around each iron atom. The first shell peak is similar in shape for the Fe(Cl(PDC)) dimer, which contains a linear μ-oxo bridge, and the met and oxy forms of hemerythrin, suggesting a μ-oxo bridge in these forms of hemerythrin. To interpret the met- and oxyhemerythrin data we used the $\chi(k)$ from the Fe(glycine) and Fe(TIM) standards to obtain the backscattering amplitudes from oxygen and nitrogen atoms, respectively. A nonlinear, least-squares fitting technique was then employed to match the calculated $\chi(k)$ to the measured one. Guided by the X-ray results,[6] the first shell in hemerythrin was modeled by three nitrogen and two oxygen atoms at a single average distance modified by a Debye–Waller factor to account for a spread in the distances about the mean.[16] To this were added the signal for a single oxygen atom at a shorter distance and a different Debye–Waller factor. The program was then allowed to vary the two distances and the two Debye–Waller factors to minimize the differences in phase and amplitude between the manufactured signal and the hemerythrin first-shell data.

The results of the first-shell fitting for oxy- and methemerythrin and the Fe(Cl(PDC)) dimer are shown in Table II, and a sample fit is shown in Figure 5. The validity of the fitting procedure is proven by the excellent agreement between the EXAFS values and the X-ray diffraction values for the Fe(Cl(PDC)) dimer. Although the fits are not very sensitive to the number of nitrogen vs. oxygen ligands (keeping the total at five), the program tended to prefer one-half more oxygen atom and one-half less nitrogen atom for oxyhemerythrin than for metazidohemerythrin. Since the EXAFS signal represents an average of the two iron atoms at the active site, this result is consistent with the replacement of the exogenous nitrogen ligand by oxygen at one of the two iron atoms in oxyhemerythrin. The deoxyhemerythrin data will be considered under Discussion.

Third Coordination Shell. The third EXAFS peak (Figure 4) is present in all of the hemerythrin samples but is absent from

(17) Stern, E. A.; Sayers, D. E.; Lytle, F. W. *Phys. Rev. B: Solid State* **1975**, *11*, 4836–4846.
(18) Lee, P. A.; Pendry, J. B. *Phys. Rev. B: Solid State* **1975**, *11*, 2795–2811.
(19) Teo, B. K. *J. Am. Chem. Soc.* **1981**, *103*, 3990–4001.

Table II. First-Shell Fits for Hemerythrins and Fe(Cl·PDC) Dimer

compound	five ligand set (3N, 2O)[a] average distance, Å	five ligand set (3N, 2O)[a] Debye-Waller factor, Å	bridging oxygen distance, Å	bridging oxygen Debye-Waller factor,[b] Å
		EXAFS		
Fe(Cl·(PDC)) dimer	2.10 ± 0.05	0.0003 ± 0.001	1.79 ± 0.05	−0.005 ± 0.005
metazidohemerythrin	2.15 ± 0.05	0.005 ± 0.001	1.80 ± 0.05	−0.002 ± 0.005
methydroxohemerythrin	2.15 ± 0.05	0.007 ± 0.001	1.82 ± 0.05	−0.004 ± 0.005
oxyhemerythrin	2.16 ± 0.05	0.005 ± 0.001	1.83 ± 0.05	−0.003 ± 0.005
		Crystallographic Results		
Fe(Cl·(PDC)) dimer[c]	2.08	0.0005	1.77	

[a] Fe(glycine) trimer and Fe(TIM) compound were used as standards for oxygen and nitrogen contributions, respectively. Error limits include effects of varying the relative energy reference between standards and unknown and varying the relative number of nitrogen and oxygen ligands in the coordination shell. [b] Values are essentially zero because the noise is large relative to the amplitude at the high end of the spectrum. [c] Reference 11.

both of the Fe standards. A similar peak has been observed with other metalloproteins—e.g., the iron-containing photosynthetic-reaction-center protein[20] and the copper-containing hemocyanin[21] —as well as with zinc[22] and copper[23] imidazole complexes. It is assigned to scattering at the third-neighbor coordination shell around the iron from the N1 and C5 atoms of the imidazole ring. The high intensity of the signal can be explained by a combination of the focusing effect of the intervening N3 atom that is bonded to the metal and a comparatively small Debye–Waller factor.[20] Our results indicate a similar amount of histidine ligation in oxyhemerythrin, methemerythrins, and also deoxyhemerythrin. The X-ray results[6] indicate 3 histidine rings ligated to one iron and 2 ligated to the other for an average of 2.5 rings per iron.

Discussion

Structure of Oxyhemerythrin. The near-edge and EXAFS measurements provide direct evidence for the presence of a similar binuclear iron structure in oxyhemerythrin and in methemerythrins (azide and hydroxide forms). Both are characterized by ferric Fe octahedrally coordinated, as had previously been suggested on the basis of near-infrared absorption spectra.[24] With the exception of the exogenous ligand (i.e., peroxide, azide, hydroxide), both oxyhemerythrin and methemerythrins appear to have the same number and types of iron ligands and the same iron–ligand distances (Tables I and II). The iron–iron distance in metazidohemerythrin may be shorter than in the other two ferric forms. The equality of the third-shell histidine peak height in oxyhemerythrin (Figure 4) to that of all of the methemerythrins indicates the same five histidine ligands in all. The close agreement of the first-shell fits (Table II) suggests that the carboxylate and oxo group bridges must be present as well. Thus, our results are consistent with the active site of oxyhemerythrin having the structure shown in Figure 1 but with a peroxide ion in place of the azide ion and some slight rearrangement in the bridging atoms to give an increased Fe–Fe distance.

The iron atoms in oxyhemerythrin are known[25] to be strongly antiferromagnetically coupled with an exchange coupling ($-J$) of 77 cm^{-1}. Similar $-J$ values of $\sim$95 cm^{-1} are observed in Fe(III) complexes containing Fe_2O centers in which the distance between the iron and the bridging oxo group is 1.76–1.82 Å. Considerably smaller $-J$ values of $\sim$30 cm^{-1} are observed[26] in Fe_3O complexes in which the iron–oxygen distance has increased to 1.92–1.96 Å. According to our EXAFS measurements (Table II), the separation between the iron and the bridging oxygen in oxyhemerythrin is 1.83 ± 0.05 Å. This distance is close to distances found in the Fe_2O complexes and thus is expected to result in strong antiferromagnetic coupling of the iron atoms. Our results indicate that even though the iron atoms in oxyhemerythrin are triply bridged by one oxo and two carboxylates as in the Fe_3O-containing complexes, the actual Fe–O–Fe bond structure and chemistry are closer to those of the singly bridged Fe_2O-containing complexes. The short length of the Fe–O bond in oxyhemerythrin means that the antiferromagnetism of its binuclear iron center can be ascribed chiefly to the μ-oxo bridge with little contribution from the bridging carboxylates, as is also the case in the oxo-bridged model complexes.[26]

Fe–O–Fe Geometry. The X-ray scattering amplitude is generally enhanced by intervening atoms that are directly in the path between the absorber and the backscatterer.[18,19] Thus, the Fe-(Cl(PDC)) dimer (with an Fe–O–Fe angle of 180°)[11] shows a twofold enhancement in iron scattering amplitude relative to the Fe(glycine) trimer (with an Fe–O–Fe angle of 120°)[27] and the iron foil (with no intervening atoms). Our data for oxy- and methemerythrin show no such enhancement, leading to the conclusion that the bridging oxygen is not precisely on the line between the two iron atoms. Use of the bond distances listed Tables I and II give the Fe–O–Fe angles listed in Table I. Unfortunately, the uncertainty is too large to exclude 180°. However, all the angles are consistent with being small enough to have no amplitude enhancement. This geometry is similar to that observed in $[Fe_2O\cdot(HEDTA)_2]^{2-}$, where the Fe–O–Fe angle is 165°.[28] The EXAFS of $[Fe_2O\cdot(HEDTA)_2]^{2-}$ has been measured by two groups. Hendrickson et al.[29] have found that both the amplitude and the phase shift of the iron–iron peak are altered by the intervening oxygen in such a manner as to make the distances obtained from EXAFS *shorter* than the crystallographic distances. Alberding,[30] however, obtains the same distance as that in crystallography by conventional EXAFS analysis of his data. We have reanalyzed Alberding's data and also agree with the crystallographic distance to within our errors. The Fe–Fe distance would be increased, and Fe–O–Fe geometry assigned to hemerythrin would be considerably altered if our protein samples and model compounds were affected by the intervening O in the way Hendrickson et al. have observed.

The iron–iron distance of 3.49 ± 0.08 Å that we have determined for metazidohemerythrin does not agree well with the present crystallographic estimate of 3.30 Å.[31] Although the positions of heavy atoms should be accurately measurable by X-ray crystallography, this has proved to be difficult in the case of hemerythrin. Original estimates of the iron–iron distance by this

(20) Bunker, G.; Stern, E. A.; Blankenship, R. E.; Parson, W. W. *Biophys. J.* **1982**, *37*, 539–551.
(21) Co, M. S.; Hodgson, K. O.; Eccles, T. K.; Lontie, R. *J. Am. Chem. Soc.* **1981**, *103*, 984–986.
(22) Azoulay, J., private communication.
(23) Co, M. S.; Scott, R. A.; Hodgson, K. O. *J. Am. Chem. Soc.* **1981**, *103*, 986–988.
(24) Loehr, J. S.; Loehr, T. M.; Mauk, A. G.; Gray, H. B. *J. Am. Chem. Soc.* **1981**, *102*, 6992–6996.
(25) Dawson, J. W.; Gray, H. B.; Hoenig, H. E.; Rossman, G. R.; Schredder, J. M.; Wang, R.-H. *Biochemistry* **1972**, *11*, 461–465.
(26) Thich, J. A.; Toby, B. H.; Powers, D. A.; Potenza, J. A.; Schugar, H. J. *Inorg. Chem.* **1981**, *20*, 3314–3317.
(27) Thundathil, R. V.; Holt, E. M.; Holt, S. L.; Watson, K. J. *J. Am. Chem. Soc.* **1977**, *99*, 1818–1823.
(28) Lippard, S. J.; Schugar, H.; Walling, C. *Inorg. Chem.* **1967**, *6*, 1825–1831.
(29) Hendrickson, W. A.; Smith, J. L.; Co, M. S.; Hodgson, K. O., private communication.
(30) Alberding, N., private communication.
(31) Stenkamp, R. E.; Sieker, L. C.; Jensen, L. H., private communication.

technique (at 2.8 Å resolution) ranged from 3.44 Å in metazidomyohemerythrin[32] to 3.05 Å in metaquohemerythrin.[4] It appears that it is going to be equally difficult to determine an accurate iron–iron distance with EXAFS. Hendrickson et al.[29] have EXAFS data indicating that the iron–iron separation in metazidohemerythrin is less than the 3.32-Å value for the oxo-bridged trimer $[Fe_3O(SO_4)_6(H_2O)_3]$. However, our EXAFS data (Table I) show that the iron–iron spacing in metazidohemerythrin is considerably longer than the 3.30 Å of the Fe(glycine) trimer. This discrepancy is outside our error limits, which are based on pairwise comparisons between hemerythrin, the Fe(Cl(PDC)) dimer, iron foil, and Fe(glycine) trimer. Further investigations are clearly needed to reconcile these differences.

Structure of Deoxyhemerythrin. The binuclear iron center of deoxyhemerythrin is shown also to possess octahedral iron coordination by the weakenss of the 3d pip in its near edge (Figure 2), in agreement with its near-infrared spectrum.[24] Furthermore, the histidine ligands from the protein backbone appear to be intact on the basis of the EXAFS peak from the third-shell atoms (Figure 4). However, the first-shell geometry is obviously quite different from the other forms. The EXAFS data indicate the loss of the μ-oxo bridge, in agreement with the observed lack of antiferromagnetic coupling between the irons in deoxyhemerythrin.[2] This loss is evident in three ways. The 3d pip in deoxyhemerythrin is smaller than in the ferric forms, consistent with the replacement around each iron of a single short bond by a more inversion-symmetric environment. More dramatic is the disappearance of the Fe–Fe peak in the transforms of Figure 4. Finally, the first-shell EXAFS data are different in the deoxy form from that of the other forms and from the Fe(Cl(PDC)) dimer.

The loss of the iron–iron peak in deoxyhemerythrin may indicate that there has been enough change in the distance of the iron atoms to cause the iron–iron signal to become buried under some other signal. This seems unlikely in view of the unaltered histidine EXAFS signal and the fact that crystals of deoxyhemerythrin can be converted to oxyhemerythrin without any change in crystal morphology.[31] Since the two iron atoms in hemerythrin are sandwiched between four α helices,[4] the 2-Å movement of the iron atoms required by this explanation would surely have caused a marked disruption in the polypeptide backbone orientation. An alternative explanation is that in the absence of the μ-oxo bridge the iron atoms undergo uncorrelated thermal vibrations that reduce the iron–iron signal to below the signal-to-noise ratio. Previous work on model compounds with multiple metal centers has indicated that metal–metal interaction is more likely to be detected by EXAFS when there is strong bridging between the metal atoms.[33] We plan to make more extensive measurements on deoxyhemerythrin as a function of temperature to test the above possibility. We will also attempt to find standards whose EXAFS more closely resemble that of deoxyhemerythrin and reserve our detailed analysis of the data until these experiments have been completed.

Conclusions

EXAFS measurements on deoxy-, oxy-, and methemerythrins have helped elucidate structural similarities and differences between them. There is now direct evidence that oxyhemerythrin has a similar structure to metazidohemerythrin and methydroxohemerythrin, differing in the nature of the bound anion. Although the iron–iron spacing from these measurements is somewhat longer than that measured by X-ray crystallography, the basic structure proposed by the latest crystallographic measurements[6] is supported. The data on deoxyhemerythrin show that while the histidine ligation has been retained, the EXAFS departs significantly from the other forms of hemerythrin. The iron–iron signal has disappeared, showing the loss of the bridging oxo group, and the first-shell distances other than the histidine nitrogen are rearranged.

Acknowledgment. We are pleased to acknowledge the advice and stimulating discusions with Drs. W. W. Parson, T. M. Loehr, R. E. Stenkamp, and L. H. Jensen. W.T.E. is indebted to James Collman, Eric Evitt, Bob Kreh, and Craig Barnes of the Stanford University Chemistry Department for assistance in handling oxygen-free samples. The research reported here was supported by the National Science Foundation (Grant PCM 79-03674) and the National Institutes of Health (Grant GM18865). The support and help of the staff of SSRL was essential in conducting these experiments. SSRL is supported by the National Science Foundation through the Division of Materials Research and the National Institutes of Health through the Biotechnology Resource Program in the Division of Research Resources in cooperation with the Department of Energy.

Registry No. Fe, 7439-89-6.

(32) Hendrickson, W. A.; Klippenstein, G. L.; Ward, K. B. *Proc. Natl. Acad. Sci. U.S.A.* **1975**, 2160–2164.

(33) Cramer, S. P.; Hodgson, K. O.; Stiefer, E. I.; Newton, E. W. *J. Am. Chem. Soc.* **1978**, *100*, 2748–2761.

Electrochemistry in Liquid Sulfur Dioxide. 3. Electrochemical Production of New Highly Oxidized 2,2′-Bipyridine Complexes of Ruthenium and Iron

John G. Gaudiello, Paul R. Sharp, and Allen J. Bard*

Contribution from the Department of Chemistry, The University of Texas at Austin, Austin, Texas 78712. *Received February 24, 1982*

Abstract: The electrochemical oxidation of $Ru(bpy)_3^{2+}$ and $Fe(bpy)_3^{2+}$ in liquid sulfur dioxide was investigated. $Ru(bpy)_3^{2+}$ shows two oxidation waves corresponding to the 3+ (1.01 V) and 4+ (2.76 V) forms while $Fe(bpy)_3^{2+}$ undergoes three oxidations to the 3+ (0.70 V), 4+ (2.92 V), and 5+ (~3.09 V) forms. While the 3+ form is stable for both compounds on a coulometric time scale, the higher oxidation states react with solvent to regenerate the 3+ form. The kinetics of this reaction was studied as a function of temperature by cyclic voltammetry, chronocoulometry, and chronoamperometry.

Introduction

Liquid sulfur dioxide containing a suitable electrolyte (e.g., tetra-*n*-butylammonium perchlorate, TBAP) has been shown to be a useful solvent for electrochemical studies, especially in the region of very positive potentials where strongly oxidizing species can exist.[1,2] Thus the limit for background oxidation with 0.1

0002-7863/82/1504-6373$01.25/0